# Hybrid simulation of an old reinforced concrete viaduct based on nonlinear substructuring techniques

G. Abbiati[1], O.S. Bursi[1], E. Cazzador[1], R. Ceravolo[2], and Z. Mei[1,3]

[1]University of Trento, Dep. of Civil, Environmental and Mechanical Engineering, Trento, Italy
[2]Polytechnic of Turin, Dep. of Structural, Geotechnical and Building Engineering, Turin, Italy
[3]Harbin Institute of Technology, School of Civil Engineering, Harbin, China

ABSTRACT: The seismic performance assessment of an underdesigned 400m span viaduct was conceived within the RETRO TA of the SERIES European project by means of Continuous-Time Hybrid Simulations (CTHS). In detail, two of the twelve piers - Physical Substructures (PS) - will be loaded through dynamic actuators at the Joint Research Centre of Ispra, Italy, whilst the remainder ten piers and the deck as well - Numerical Substructures (NSs) - will be simulated numerically. Time history analyses conducted on a refined OpenSEES fiber based Finite Element (FE) model of the bridge highlighted hysteretic energy dissipation within piers already at the serviceability limit state. Nonetheless, the typical solving time of the NS dictated by the experimental equipment - few milliseconds - make complex nonlinear FE models not suitable for testing purposes. In order to circumvent this strict testing limitation, a rational design of NSs based on model reduction techniques is proposed.

*Keywords: Hybrid simulations; model reduction; seismic assessment; OpenSEES.*

## 1 INTRODUCTION

A full-scale testing program was conceived within the RETRO Transnational Activity, of the SERIES research project (Taucer, 2011, Abbiati et al, 2013). The case study consists of an old concrete viaduct, where two independent roadways are supported by 12 couples of portal piers composed of two circular columns of variable diameter comprised between 1.20m÷1.60m. According to Figure 1, one or more transverse beams endowed with rectangular cross section connect each couple of columns at different levels. The height of the piers range between 13.80 -near the abutments- and 41.00m -in the middle of the bridge-. Six Gerber saddles interrupt the reinforced concrete beams of the deck characterized by 33m fixed length bays, expect for the extreme spans, which measure 29m. The linear distributed dead load of the deck of about 170kN/m per roadway entails a constant vertical load equal to 5600kN on each pier. Two vertical steel bars connect the deck to each pier portal frame.

Figure 1a. Views of the Rio Torto viaduct portal piers

Figure 1b. Views of the Rio Torto viaduct concrete decks

A comprehensive set of CTHS was conceived to estimate the seismic performance of the bridge. In detail, two of the twelve piers - (PSs) - will be loaded through dynamic actuators at the Joint Research Centre of Ispra (JRC), Italy, whilst the remainder and the deck as well - (NSs) - will be numerically modelled and solved. First, the experimental set-up is described; in detail, the specimens are presented and both the NS and PS are characterized as well as the seismic input. In order to support the design of the NS, an OpenSEES FE fiber based FE Reference Model (RM) of the bridge is then introduced. Time history analyses conducted on the aforementioned OpenSEES RM highlighted appreciable nonlinearities in the dynamic response of piers already under the Serviceability Limit State (SLS). As a consequence, a NS capable of reproducing this nonlinear behaviour during CTHS was deemed necessary. In this perspective, a rational model reduction of nonlinear numerical piers was conceived as an extension of the Guyan method (Guyan, 1965); in order to reproduce the hysteretic behaviour of refined fiber-based piers, a 3-DoFs superelement resulting from the linear dynamic substructuring of each single pier was endowed with a modified Bouc-Wen spring with softening behaviour. Lastly, the numerical validation of the reduced model of the viaduct is presented and commented.

## 2 DESCRIPTION OF HYBRID SIMULATIONS

According to the foreseen experimental set-up, two of the twelve piers -PSs- will be loaded through dynamic actuators at JRC) whilst the remaining ten piers and the deck as well -NSs- will numerically modelled and solved. Figure 2 depicts the whole emulated system. Piers #9 and #11, are highlighted as PSs.

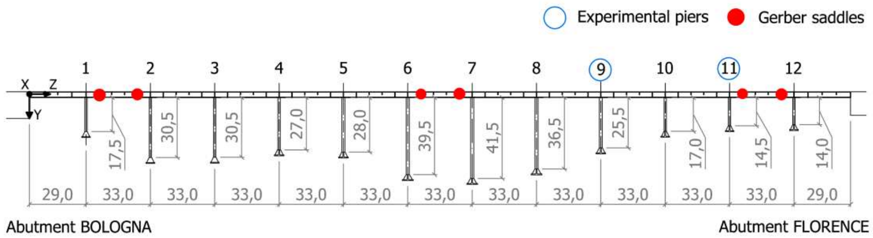


Figure 2. Structural scheme and main dimensions (in m) of the Rio Torto viaduct

Figure 3 depicts the experimental set-up of the mock-up 1:2.5 scale specimen of Pier #11.

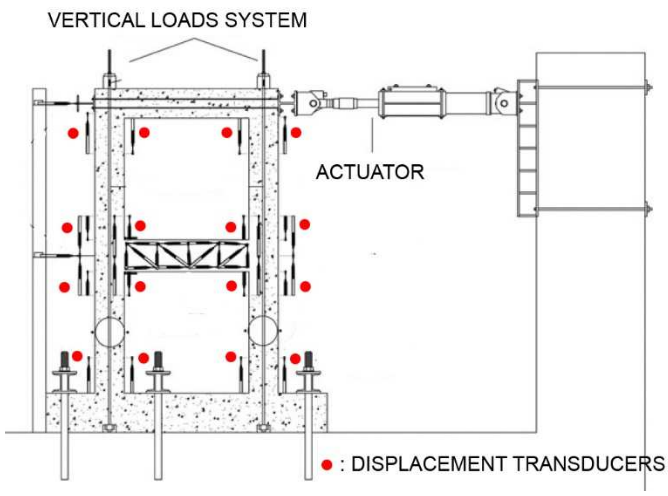


Figure 3. Experimental set-up relevant to Pier #11

Two seismic records of the Emilia (Italy) earthquake of the 29th of May 2012 were considered to reproduce the Serviceability Limit State (SLS) and the Ultimate Limit State (ULS), respectively. In detail, records from the Mirandola station were selected because of their seismological characteristics, i.e. PGA and duration. As a result, the East-West component of the earthquake was considered for the SLS (2.56 $m/s^2$ PGA), whilst the North-South component was assumed for the ULS (2.67 $m/s^2$ PGA). Both for the W-E and N-S accelerograms, a significant amplification was observed for low periods, i.e. between 0.50 and 1.00s. Nonetheless, just the NS component exhibited spectral accelerations of about 0.40g also in the period range from 1.00 to 1.50s as depicted in Figure 4b.

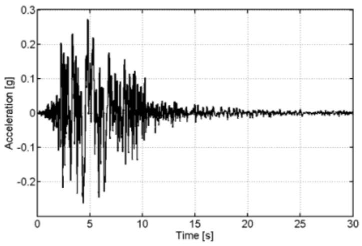


Figure 4a - Accelerogram of the N-S component of the Emilia earthquake selected for the ULS

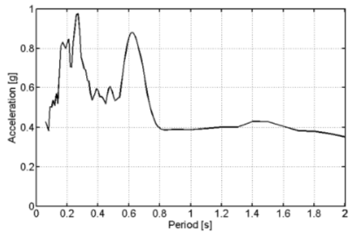


Figure 4b – Acceleration response spectrum of the N-S component of the Emilia earthquake selected for the ULS

In this context, the PM interfield-parallel time integration algorithm (Pegon and Magonette 2002, Bonelli et al. 2008) will be implemented; thanks to the subcycling capabilities of the PM method, the complex nonlinear NS is handled with a coarse time step, whilst the PS advances with the controller time step.

## 3 OPENSEES REFERENCE MODEL OF THE BRIDGE

In order to support the test design (Paolacci and Giannini, 2011), the OpenSEES RM able to simulate the hysteretic behaviour of piers was set. The Kent-Scott-Park model was employed to emulate the concrete behaviour (Kent and Park, 1971). Conversely, the Menegotto-Pinto model was adopted for steel reinforcements (1973). As a result, the *Concrete01* OpenSEES material was considered for concrete, whilst the *Steel02* OpenSEES material was adopted to model steel reinforcements. The piers were considered clamped at the base, whilst the abutments were released along the longitudinal direction of the bridge at both sides. In order to take into account the offset distance between the center of gravity of the deck cross section and the cap beam axis, each pier was connected to the deck through a rigid link, which was considered fixed to the deck and hinged to the relevant pier, as shown in Figure 5.

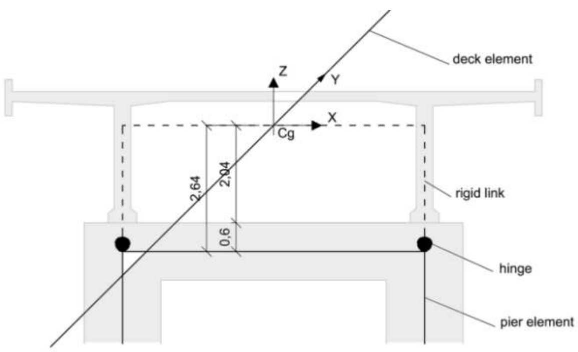


Figure 5. Details of the FE modelling of the pier-deck connection (Dimensions in m)

Both the flexural and the transverse beam shear nonlinear behaviours were taken into account, whilst the fix-end rotation effects owing to strain-penetration of steel bars was neglected. Since this refined fiber-based FE model was capable of reproducing the complex behaviour of the full emulated system, a comprehensive set of time history analyses was carried out to simulate the dynamic response of the bridge at different limit states. Figures 6a and 6b report the hysteretic loops relevant to Piers #9 and #11 (PSs) for the SLS; each transversal displacement was measured at the cap beam level, whilst the base reaction in the same X direction was considered by the plots.

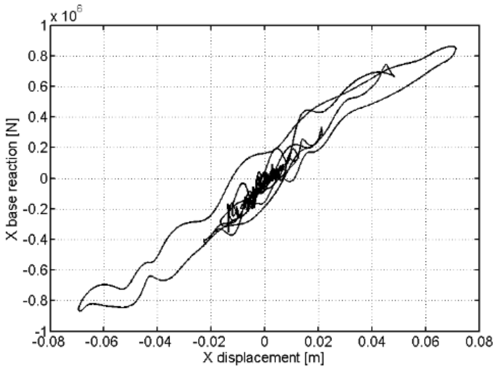


Figure 6a. Transversal base reaction hysteretic loop relevant to Pier #9

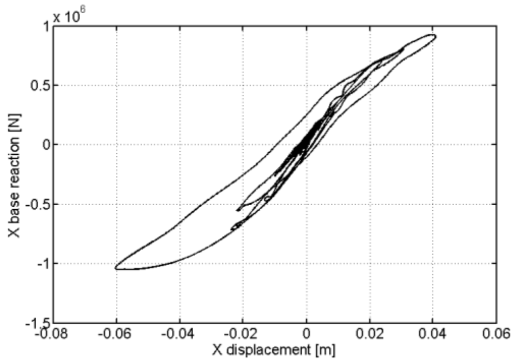


Figure 6b. Transversal base hysteretic loop relevant to Pier #11

According to Figure 6, nonlinearities in the dynamic response can be appreciated already at SLS. In principle, hysteretic loops of tall piers, such as Pier #9, are more jagged that the ones relevant to short piers, such as Pier #11.

## 4 NONLINEAR SUBSTRUCTURING OF HYSTERTIC PIERS

Since OpenSEES does not provide tangent stiffness and mass matrices, a Linear ANSYS Model (LM) of the bridge was produced. Aforementioned matrices were imported in MatLAB where the model reduction of piers was performed. According to Table 1, modal analyses proved the consistency between the different models of the Rio Torto Viaduct in the linear range.

Table 1. Modal analysis of the FE model of the bridge

| Mode | OpenSEES RM nonlinear model [Hz] | ANSYS LM linear model [Hz] |
|---|---|---|
| 1 | 0.6035 | 0.6254 |
| 2 | 0.6590 | 0.6452 |
| 3 | 0.6687 | 0.7017 |
| 4 | 1.1763 | 1.1023 |
| 5 | 1.2822 | 1.2183 |

In view of an optimal substructuring of each pier, a deep study was focused on the internal constraint setting of the resulting 832 DoFs ANSYS LM. Since neither torsional nor out-of-plane bending eigenmodes of piers were excited, relative rotations between the deck and piers were released, whilst out-of-plane displacements of piers were fixed. A modified ANSYS model embedding the new constraints was set accordingly. Figure 7a and 7b compare the primal and the modified constraint settings.

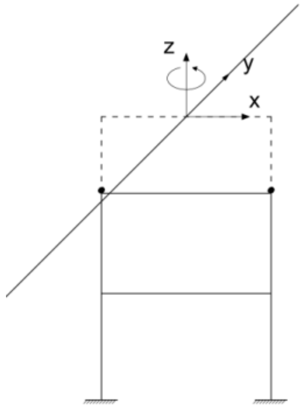


Figure 7a - Primal constraint setting

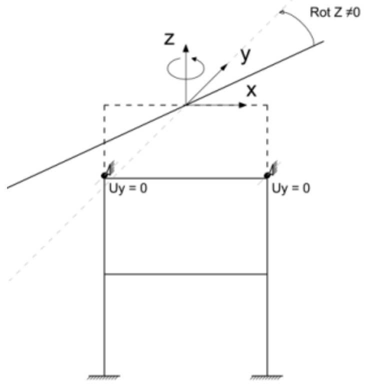


Figure 7b - Modified constraint setting

As a result, each pier was condensed to a plane superelement. As shown in Figure 9, the in-plane interface displacement DoFs shared with the relevant rigid link element, which provided the connection to the deck, were retained.

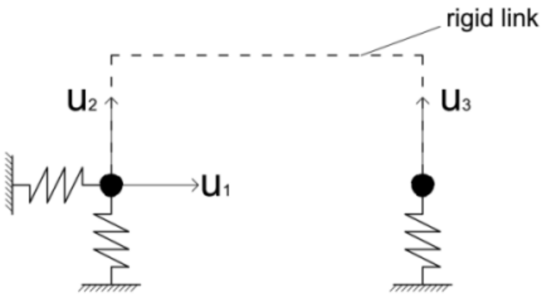


Figure 9 - Pier 3-DoFs superelement geometry

The resulting 3-DoFs pier superelements was obtained with the well-known Guyan method (Guyan, 1965). The linear transformation leading to reduced matrices reads:

$$[\mathbf{u}] = \begin{bmatrix} \mathbf{u_R} \\ \mathbf{u_L} \end{bmatrix} = \begin{bmatrix} \mathbf{I} \\ \mathbf{\Phi_R} \end{bmatrix} \cdot [\mathbf{u_R}] = [\mathbf{T}] \cdot [\mathbf{u_R}] \tag{1}$$

where $\mathbf{u_R}$ defines master DoFs; $\mathbf{u_L}$ determines slave DoFs; and $\mathbf{\Phi_R}$ defines the boundary node functions. Each boundary node function corresponds to the deformed static configuration of the model being substructured resulting from the application of a unitary displacement to one master DoF with the others kept fixed. According to the Craig-Bampton method (Craig, Bampton, 1968), in-plane fixed-end local eigenmodes of piers might be considered if excited, as a further refinement of the linear substructuring, but this was not the case. The ANSYS LM provided with Guyan-based reduced piers well agrees with the ANSYS LM. Figures 10a and 10b compare the dynamic responses of Pier #1 in terms of transversal displacement at the cap beam level.

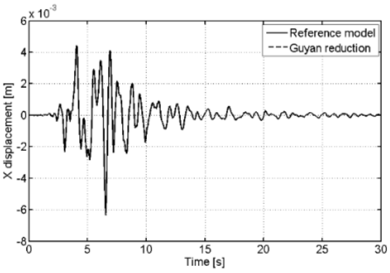


Figure 10a - Transversal displacement response of Pier #1 measured at the cap beam level

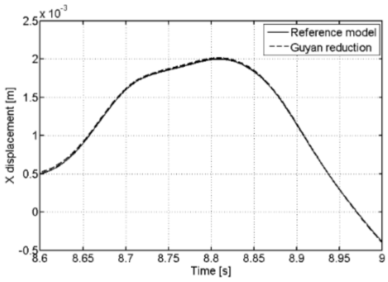


Figure 10b- Zoom on a peak of the transversal displacement response of Pier #1 measured at the cap beam level

In view of a model reduction of each single hysteretic nonlinear pier, the $k_{11}$ element of the $\mathbf{K}$ matrix was replaced with a modified Bouc-Wen spring with softening behaviour. The restoring force vector relevant to the master DoFs of each substructured pier was expressed in terms of an extended state space formulation based on an extended state space vector, which reads:

$$[\mathbf{r}]=[\mathbf{K}][\mathbf{u_R}]=\begin{bmatrix}k_{11} & k_{12} & k_{13}\\ k_{21} & k_{22} & k_{23}\\ k_{31} & k_{32} & k_{33}\end{bmatrix}\begin{bmatrix}u_{R,1}\\ u_{R,2}\\ u_{R,3}\end{bmatrix}\Rightarrow\begin{bmatrix}r_1\\ r_2\\ r_3\end{bmatrix}=\begin{bmatrix}0 & k_{12} & k_{13}\\ k_{21} & k_{22} & k_{23}\\ k_{31} & k_{32} & k_{33}\end{bmatrix}\begin{bmatrix}u_{R,1}\\ u_{R,2}\\ u_{R,3}\end{bmatrix}+\begin{bmatrix}f_1\\ 0\\ 0\end{bmatrix} \tag{2}$$

$$\dot{f}_1=\left(\rho\cdot A\Big/\left(1+a\cdot u_{R,1}^2\right)-(\beta\cdot sgn(\dot{u}_{R,1}\cdot f_1)+\gamma)\,|\,f_1\,|^n\right)\cdot\dot{u}_{R,1} \tag{3}$$

where $A$, $\beta$, $\gamma$ and $n$ are the parameters of the Bouc-Wen model. $A$ was assumed equal to $k_{11}$ element of the linear initial tangent stiffness matrix, whilst $\rho$ was introduced to represents its average degradation. Since the reduction of the global bridge entails the tuning of all the twelve piers, to decrease the computational burden of the resulting set of optimization problems γ was set to zero and the $n$ to one. The softening factor depending on the α parameter was introduced according to the material properties of the OpenSEES RM. As highlighted by Bursi et al. (2012), $\dot{f}_1$ is homogeneous of order one with respect to $\dot{x}_1$, and therefore, $f_1$ is rate-independent; this feature complies well with conventional PsD tests, where strain-rate effects are neglected. It is evident from Eq. (2) that we are neglecting the nonlinearities in the vertical springs of Figure 9. They could be taken into account thanks to the Wang and Chang treatment (Wang and Chang, 2007). Table 2 summarized identified parameters values, which clearly depend on the excitation level.

Table 2. Bouc-Wen springs with softening behaviour parameters

| Pier | SLS | | | ULS | | |
|---|---|---|---|---|---|---|
| | ρ | a | β | ρ | a | β |
| 1 | 1,00 | 198,71 | 0,00 | 0,55 | 199,59 | 0,66 |
| 2 | 0,82 | 54,70 | 1,54 | 0,50 | 0,03 | 0,94 |
| 3 | 0,88 | 89,58 | 1,36 | 0,50 | 0,05 | 0,84 |
| 4 | 0,64 | 61,54 | 1,46 | 0,52 | 37,06 | 1,23 |
| 5 | 0,64 | 78,23 | 1,63 | 0,50 | 28,69 | 1,24 |
| 6 | 0,86 | 84,01 | 1,14 | 0,61 | 0,06 | 0,82 |
| 7 | 0,67 | 10,06 | 0,92 | 0,59 | 6,30 | 0,53 |
| 8 | 0,75 | 48,30 | 0,68 | 0,70 | 34,13 | 1,24 |
| 9 | 0,78 | 191,34 | 1,19 | 0,50 | 23,00 | 1,00 |

| | | | | | | |
|---|---|---|---|---|---|---|
| 10 | 0,99 | 199,06 | 0,00 | 0,53 | 165,58 | 1,58 |
| 11 | 0,66 | 175,68 | 1,05 | 0,50 | 193,81 | 2,50 |
| 12 | 0,91 | 198,86 | 0,02 | 0,56 | 199,60 | 0,00 |

A time-domain approach was applied for the identification of the parameters. In detail, the Matlab patternsearch algorithm was selected to minimize the error norm defined on OpenSEES RM transversal displacement signals. According to the engineering sense, an appreciable degradation of initial elastic tangent stiffness can be appreciated in the transition between SLS and ULS.

## 5 VALIDATION OF THE REDUCED MODEL

The resulting reduced model based on 3-DoFs pier superelements was validated through time history analyses for both the limit states foreseen for hybrid simulations. With regard to Pier #9, Figures 11a and 11b compare the transversal displacement responses of the reduced model and the OpenSEES RM. For both the limit states, the global response of the bridge is well preserved toward the first stronger peaks whilst a slight degradation of the displacement matching occurs after the first ten seconds.

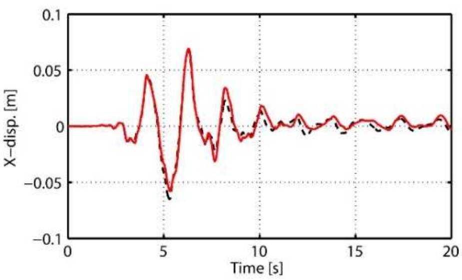


Figure 11a. Transversal displacement response of pier #9 measured at the cap beam level at SLS

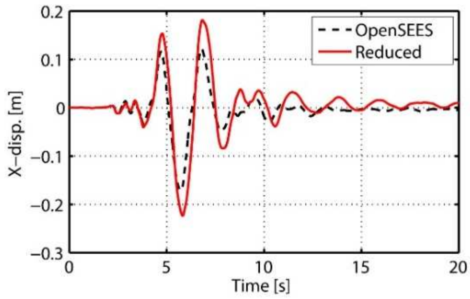


Figure 11b. Transversal displacement response of pier #9 measured at the cap beam level at ULS

With respect to the OpenSEES RM, a Normalized Root Mean Squared Error (NRMSE) was introduced as a dimensionless error measure on transversal kinematic quantities, such as displacement, velocity and acceleration, measured at the cab beam level of each single pier. Relevant values are summarized in Table 3.

Table 3. NRMSEs on kinematic quantities measured at the cap beam level of each pier for both the LSs

| Pier | SLS | | | ULS | | |
|---|---|---|---|---|---|---|
| | Disp. [m] | Vel. [m/s] | Acc. [m/s$^2$] | Disp. [m] | Vel. [m/s] | Acc. [m/s$^2$] |
| 1 | 0,06 | 0,06 | 0,06 | 0,11 | 0,06 | 0,04 |
| 2 | 0,05 | 0,05 | 0,05 | 0,07 | 0,06 | 0,03 |
| 3 | 0,05 | 0,05 | 0,05 | 0,06 | 0,05 | 0,03 |
| 4 | 0,05 | 0,05 | 0,05 | 0,06 | 0,05 | 0,03 |
| 5 | 0,05 | 0,05 | 0,05 | 0,06 | 0,05 | 0,03 |
| 6 | 0,05 | 0,05 | 0,05 | 0,06 | 0,05 | 0,03 |
| 7 | 0,03 | 0,03 | 0,03 | 0,05 | 0,03 | 0,02 |
| 8 | 0,03 | 0,03 | 0,03 | 0,05 | 0,03 | 0,02 |
| 9 | 0,03 | 0,03 | 0,03 | 0,08 | 0,03 | 0,02 |
| 10 | 0,05 | 0,05 | 0,05 | 0,13 | 0,04 | 0,02 |
| 11 | 0,04 | 0,04 | 0,04 | 0,15 | 0,04 | 0,03 |
| 12 | 0,04 | 0,04 | 0,04 | 0,08 | 0,03 | 0,02 |

NRMSEs prove the consistency between the reduced and the OpenSEES models for both the LSs.

## 6 CONCLUSIONS

The case study of the Rio Torto viaduct is presented within the framework of the RETRO TA research activity whose aim was the assessment of the seismic performance of an under designed 400m span bridge by means of CTHSs. A complex OpenSEES fiber based FE model of the viaduct was set to support the test design. Since the typical solving time of the NS dictated by the experimental equipment -few milliseconds- makes complex FE models not suitable for testing purposes, a rational design of the NS based on a rigorous reduction of the OpenSEES RM is presented. First, a linear FE ANSYS model was set to obtain stiffness and mass matrices for the dynamic reduction of piers. In order to force an in-plane response of each single pier, the constraint setting of piers-deck connections was modified. Successively, a Guyan static condensation was applied to substructured piers and a feasible extension to the nonlinear range by means of a modified Bouc-Wen spring with softening behaviour was presented. The tuning of such reduced nonlinear piers was made to preserve transversal displacements. Finally, the validation of the reduced model of the bridge is presented. According to the component synthesis approach, PSs can be easily accommodated in place of relevant numerical piers.

## 7 ACKNOWLEDGEMENT

The authors greatly acknowledge the financial support from the European Union through the SERIES projects (Grant number: 227887). Nonetheless, opinions are those of the author.

## 8 REFERENCES

Abbiati G, Bursi O.S., Cazzador E., Mei Z., Paolacci F., Pegon P., 2013. Pseudo-dynamic testing with non-linear substructuring of a reinforced concrete bridge based on system identification and model updating techniques. SERIES Concluding Workshop joint with NEES-US “Earthquake Engineering Research Infrastructures”, JRC Ispra, May 28-30.

Bonelli A.,Bursi O.S., He L., Magonette G., Pegon P., (2008). Convergence analysis of a parallel interfield method for heterogeneous simulations with substructuring. I.J.N.M.E., 75, 7, 800-825.

Bursi, O.S., Ceravolo, R., Erlicher, S., Zanotti Fragonara, L., 2012. "Identification of the hysteretic behaviour of a partial strength steel-concrete moment-resisting frame structure subject to pseudo-dynamic tests", Earthquake Engineering & Structural Dynamics, | DOI: 10.1002/eqe.2163, in press.

Craig R. and Bampton M. (1968). Coupling of substructures in dynamic analysis, AIAA, N. 6.

Guyan J. (1965) Reduction of stiffness and mass matrices. AIAA,N. 3.

Kent DC, Park R. (1971) Flexural members with confined concrete. J. S.D., ASCE, N. 97,1969–1990.

MATLAB version 2011b, 2011, computer software, The Mathworks Inc., Natick, Massachusetts.

Menegotto M, Pinto PE. (1973) Method of Analysis for Cyclically Loaded R.C. Plane Frames Including Change in Geometry and Non-Linear Behavior of Elements under Combined Normal Force and Bending. Proc. of IABSE Symposium, Vol.13, 1973; 15–22.

OpenSees, 2009, “Open System for Earthquake Engineering Simulation” http://opensees.berkeley.edu.

Paolacci F., Giannini R., (2011). An experimental and numerical investigation on the cyclic response of a portal frame pier belonging to an old reinforced concrete viaduct, Earthquake Engineering & Structural Dynamics, DOI: 10.1002/eqe.1175

Pegon P. and Magonette G., (2002). Continuous PSD testing with nonlinear substructuring: presentation of a stable parallel inter-field procedure. Technical Report 1.02.167, E.C., JRC, ELSA, Ispra, Italy.

Taucer F., (2011). Seismic Engineering Research Infrastructures for European Synergies: Activities of the Joint Research Centre in large scale experimental testing within the framework of the Eurocodes, 7$^{th}$ International conference on structural defects and rehabilitation, 2-4 June, Fortaleza, Brazil.

Wang C.H., Chang S.Y. (2007). Development and Validation of a Generalized Biaxial Hysteresis Model. Journal of Engineering Mechanics. DOI: 10.1061/ASCE0733-9399 2007 133:2 141